EPJ B
Condensed Matter and Complex Systems
EPJ.org
your physics journal

Eur. Phys. J. B (2013) 86: 390 DOI: 10.1140/epjb/e2013-40153-9

Extinction avoidance by aggregation in excitable kinetics

Sergio E. Mangioni

edp sciences
Società Italiana di Fisica
Springer

Eur. Phys. J. B (2013) 86: 390
DOI: 10.1140/epjb/e2013-40153-9

THE EUROPEAN PHYSICAL JOURNAL B

Regular Article

Extinction avoidance by aggregation in excitable kinetics

Sergio E. Mangioni[a]

IFIMAR (Universidad Nacional de Mar del Plata and CONICET), Dean Funes 3350, B7602AYL Mar del Plata, Argentina

Received 22 February 2013 / Received in final form 20 June 2013
Published online 23 September 2013 –

Abstract. We considerer that a population of individuals governed by the Nagumo model is subjected to a crisis that stimulates a predisposition towards aggregation. We assume that this trend is based on the physical mechanisms of attraction between individuals. Then we describe the post-crisis dynamics and find possible states of survival (stationary solutions). We see a dynamic rich in options with several possible survival responses.

1 Introduction

Under circumstances perceived as "normal", a population of "identical" individuals (disregarding hierarchical structures like families, tribes or others arising out of relationships of power) tends to distribute themselves homogeneously over the available portion of space (also assumed to provide homogeneous resource distribution). A one-dimensional, single component reaction-diffusion model with excitable kinetics, the reduced Nagumo equation [1]

$$\partial_t u = A\,(u-u_1)(u_2-u)(u-u_3) + D\,\partial_{xx}u \qquad (1)$$

with $A, D > 0$ and $0 \leq u_1 < u_2 < u_3$, yields analytical front solutions that evolve toward homogeneous states with population densities u_3 or u_1, according to the sign of $u_2 - (u_3+u_1)/2$. The case $u_1 = 0$ means extinction. If we express the Nagumo model non-linearity as a cubic polynomial, the linear term is negative and represents the decrease in the population by deaths. The quadratic term is positive and represents the sexual reproduction while the cubic term represents competition for the resource (Allee effect [2–4]). This model however, overlooks important evidence: under a crisis or threat, individuals of a given population tend to *aggregate* [5]. With this collective response they seek to increase the likelihood of survival against the unknown risk.

A clear example is provided by laboratory experiments on *Chlorella vulgaris*, eukaryotic unicellular green algae osmotrophs [6]. Once the flagellate protozoan phagotroph *Ochromonas vallescia* introduced into the biosystem, *Chlorella vulgaris* found to subsist after 10 to 20 generations, though predominantly in the form of stable colonies, constituted by eight of the original cells. When comparing to life as an individual, colonies have lost effectiveness regarding the processes of osmosis; hence access to resources has decreased as a price for minimizing risk to predation through increased size.

The aggregation can also arise from the adaptation to other conditionalites: metabolic cooperation among cluster-forming yeast allows them to grow at low densities prohibitive to growth of single-celled yeast [7]. Similar situations also occur in larger scales. For example, if the distribution of the resource and the environment in general is homogeneous and sufficient, in the permanent absence of a predator, it is expected that insects, mammals or fish also tend to a homogeneous distribution. The Nagumo model [1] offers an appropriate description for this purpose. However, when subject to the possible presence of a coexisting predator or the scarcity of the resource (adverse biotic factors), individuals tend to form stable clusters that seek to minimize the exposure to the external dangers and maximize their access to food [8–20].

Within this scenario, we should ask ourselves which is the mechanism that makes individuals come together. Phenomenon, that on the other hand, could have been created as a response to the adverse action of an external factor (e.g., emergence of a predator in the biosystem or a catastrophe that heavily limited or reduced the resource) [5]. It is clear that this response is due to different mechanisms depending on the species concerned. Numerous cases have been studied and reported, although with stable global constraints, i.e., not in a crisis scenario. They are reports that suggest a mechanism of attraction between individuals [21–24] and benefits due to aggregation [8–20].

It is argued, with some supporting circumstantial evidence, that the evolution of life and with it the species involved would have been in jumps, as a response to eventual crisis scenarios [5]. In this context, one would assume that these mechanisms of attraction and their consequential benefits have emerged in the same way.

Beyond how this happened, it seems that the response to the crisis was to propel (looking at it along a large enough time scale) a unifying force; or, to put it another way, the favoring of the survival of those individuals affected by such a mechanism of interaction that induces them to come together. What follows is a dynamic that destabilizes the homogeneous initial distribution and ends with stable groups of individuals or with extinction. A

[a] e-mail: smangio@mdp.edu.ar

dynamic that to the understanding of the authors of this paper, is interesting to describe globally by an appropriate mathematical model. We start with a situation previous to the crisis, where the dynamics of the system is described by the reduced Nagumo equation (1) with $u_1 = 0$. Then, we consider a crisis that triggers a mechanism of attraction between individuals and observe the generated dynamics. The result does not necessarily have to be the response to subsistence, we only describe the structures that stabilize when a mechanism of this kind is triggered. For example, in the case of the aforementioned experiment [6], a parameter that regulates the mechanism of attraction between individuals can determine the size of the colony; but the size that will result, according to Darwin's theory, will be determined by the competition between the predator and the colonies of different sizes; as well as, the competition between the colonies for the resource.

A circumstance to consider is that the force that induces the rapprochement between individuals must operate in a manner that prioritizes an optimal distance between them. An individual does not invade the space of another; therefore the proposed attraction must act up to a certain distance, beyond which they will repel each other. It is known that this is what happens in the aggregation of living beings [18–20,25,26]. In a previous report, a similar mechanism acting in a context defined by the Fisher model [27] has already been proposed.

First we describe the proposed model. Then we show how the attraction between individuals leads to the destabilization of a non zero population with homogeneous distribution (stable in the absence of attraction). It is true that the latter seems to run counter to survival; however, we present as evidence relevant effects of the attraction between individuals on the dynamics and stabilization of fronts, patterns, and solitons. Thus, if a crisis pushes the system from the survival basin, causing a front to move towards extinction, attraction between individuals can avoid extinction by promoting life in the form of these structures.

All the analysis is done using the technique of reaction diffusion equations modified by the effect of a current caused by the attraction between individuals. The latter is expressed in terms of a potential of the mean field caused by the set of individuals in a given point in space. We solved the equations describing the dynamics by resorting to numerical calculation[1]. We also use an analytical approach to evidence that, indeed, the attraction between individuals is that which enables the formation and stabilization of the solitons.

2 Model

In applying the Nagumo model, we consider that each individual requires a minimum vital space (a space that cannot be invaded by another individual). Thus, we define u as the coverage of the space available (with u a dimensionless variable normalized to 1). Under these conditions, the dynamic that the Nagumo model imposes can be expressed as:

$$\dot{u} = F(u) + \partial_x^2 u, \tag{2}$$

where $F(u) = u(u - \alpha b)(b - u)$. In comparison with equation (1), here we have:

1. let $u_1 = 0$ and $u_3 = b$ (uniform attractors) and $u_2 = \alpha b$ (ejector), where α is known as the *adversity factor*,
2. re-scaled t by A and x by $L_{\text{diff}} = \sqrt{\frac{D}{A}}$ (diffusion length),
3. exchanged the signs of two factors in $F(u)$.

The ejector $u = \alpha b$ marks a limit for subsistence. When u is less than this value, the system will evolve toward extinction and when it is larger, toward a population with density $u = b$. The Maxwell point (when the free energy for both attractors is equal) corresponds to $\alpha = \frac{1}{2}$ [28,29], So that when the adversity $\alpha < \frac{1}{2}$, the state $u = b$ is more favorable; and conversely, when $\alpha > \frac{1}{2}$, the more favorable state is $u = 0$ (hostile environment). Two attractors are hyperbolic points that can be connected by a solution front (heteroclinic) between $x = +\infty$ and $x = -\infty$. The front speed is constant and can be expressed as:

$$v = \pm \frac{b^4(\alpha - \frac{1}{2})}{6\int_{-\infty}^{\infty}(\partial_x u)^2 dx}, \tag{3}$$

where the sign $\pm$ indicates a front that connects $u = 0$ at $x = \mp\infty$ with $u = b$ at $x = \pm\infty$. It is observed that the front is static when $\alpha = \frac{1}{2}$; if $\alpha > \frac{1}{2}$, the front is moving toward extinction; and contrary, if $\alpha < \frac{1}{2}$ the front moves toward $u = b$. At the Maxwell point the speed of the front is zero and it can be expressed as:

$$u_{\mp}^{s} = \frac{b}{2}\left[1 \mp \tanh\frac{b}{2\sqrt{2}}(x - x_f)\right]. \tag{4}$$

Our goal is to incorporate the effect of attractive forces $f(x)$ between individuals into the Nagumo model. Our *main assumption* is that these forces do not enable individuals to interpenetrate their "vital spaces", so they must be repulsive at very short distances. Although it might seem crucial to define the range r_r at which they become repulsive, it has been proved that as far as $r_r \ll r_a \leq 1$ (in units of L_{diff}), then the average effect of the repulsive forces becomes irrelevant [27].

The aggregating current can be written as:

$$J_A(x) = \varepsilon_0\, u(1 - u)\, \partial_x U,$$

where

- parameter ε_0 represents interaction intensity,
- $u(1 - u)$ takes into accounts that the flux is proportional to the number of occupied cells and that the individuals can only migrate to "free cells of vital space" (taking place at distances $|x| \leq r_r$),

[1] The numerical scheme used in the simulations is the method of finite differences with a temporary step to fit the known numerical convergence criterion: $\frac{dt}{dx^2} < 0.5$. In particular, after corroborating that others more rigorous yield the same result, it was used: $\frac{dt}{dx^2} < 0.16$.

– we have defined the mean attracting force field on x – in fact, a *functional* of $u(x)$ – as:

$$U^{[u]}(x) = -\int \mathrm{d}x' f(x'-x)u(x').$$

Due to the *average* character of $U^{[u]}(x)$ (weighted moreover by the population $u(x)$ over "cells of vital space"), the details of $f(x)$ become less relevant than the value of the midrange r_a itself. We have tried two forms:

– a square shape $f(x) = -f_1$ for $r_r \leq |x| \leq r_a$,
– a Gaussian shape

$$f(x) = -\frac{f_o}{\sqrt{\pi}} \frac{\exp\left(-\frac{|x|^2}{r_a^2}\right)}{r_a},$$

without observing qualitatively relevant differences in our calculations.

The next step is to incorporate the effect of the attractive forces into equation (2) as $-\nabla J_A = -\partial_x J_A$:

$$\dot{u} = F(u) + \partial_{xx}u - \varepsilon_0 \partial_x \Big[u(1-u)\partial_x U\Big]. \quad (5)$$

As observed, the signs of the last two terms of the above expression are contrary, indicating competition between the agglutinative effect caused by the attractive forces and the homogenizing effect corresponding to the diffusion processes. For some constructive effect (to support the growth of any non homogeneity) to be possible it is necessary that the third term (effect of the attractive forces) exceeds the second (diffusion process) for any value of the field u, and this is only possible if $\varepsilon_0 > 4$ [27,30,31].

3 Stability of the u = b state under the attractive forces

In order to perform the linear stability analysis and other calculations described below, we write equation (5) in the form of a reaction-diffusion equation with a variable diffusion coefficient. To that end (and based solely on its mathematical similarity) we define an *effective* diffusion coefficient

$$D_{\text{eff}} = 1 - \varepsilon_0 \frac{\partial_x U}{\partial_x u} u(1-u),$$

where the first term represents real diffusion and the second one expresses the effect of the attractive forces (which create an aggregating current that opposes diffusion). Equation (5) now reads

$$\dot{u} = F(u) + \partial_x \Big[D_{\text{eff}}\, \partial_x u\Big]. \quad (6)$$

The fact that D_{eff} can be negative does not mean a violation of the second law of thermodynamics, since its role is formal.

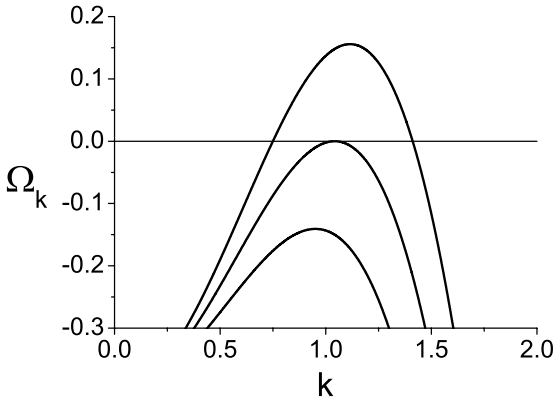

Fig. 1. Ω_k vs. k for exponential interaction. Top curve: $\varepsilon_0 = 22$, middle curve: $\varepsilon_0 = 20.013$ and down curve: $\varepsilon_0 = 18$. Other parameters: $r_a = 1$, $\alpha = 0.5$ and $b = 0.9$.

As stated above, we have tried both square and Gaussian forms of interaction between individuals. However, since the results do not provide significant differences between the two, here we only present the ones corresponding to the Gaussian form. By introducing

$$u = b + \delta\phi \exp(\Omega_k t)\exp(ikx)$$

(where $\delta\phi$ represents the amplitude of a small perturbation) into equation (6), we obtain first $\frac{\partial_x U}{\partial_x u} = \exp(-\frac{r_a^2 k^2}{4})$ and then a linearization:

$$\Omega_k = -b^2(1-\alpha) - \left[1 - \varepsilon_0 \exp\left(-\frac{r_a^2 k^2}{4}\right) b(1-b)\right] k^2, \quad (7)$$

$\Omega_k = 0$ and $\partial_k \Omega_k = 0$ determine both, the first mode that destabilizes $u = b$ (k_m) and the limit curve that separates the stable region (where the solution $u = b$ does not reach destabilization by the perturbation) from the unstable (where the solution $u = b$ is destabilized by the perturbation).

Figure 1 is a plot of Ω_k vs. k for parameter values close to the limit curve; in particular, we consider growing values of ε_0. It is noted that above a certain value of ε_0, there are a number of values of k for which a homogeneous solution is destabilized. Our calculations result in:

$$k_m^2 = \frac{-b^2(1-\alpha) + \sqrt{b^4(1-\alpha)^2 + \frac{16b^2(1-\alpha)}{r_a^2}}}{2}$$

and the limit curve

$$\varepsilon_0 = \frac{b^2(1-\alpha) + k_m^2}{k_m^2 b(1-b)} \exp\left(\frac{r_a^2 k_m^2}{4}\right).$$

Figure 2 shows the stability limit curve (SLCb, phase diagram) for ε_0 vs. b corresponding to two extreme values of r_a ($r_a = 0.001$ and $r_a = 1$). It is noted that the dominant form, even for $r_a = 1$, is that corresponding to the strongest approximation. For the particular case in that the midrange is much less than the diffusion length ($r_a \ll 1$): $k_m^2 \approx \frac{2b\sqrt{1-\alpha}}{r_a}$ and $\varepsilon_0 \approx \frac{2+r_a b\sqrt{1-\alpha}}{2b(1-b)} \approx \frac{2}{2b(1-b)}$. These approximations work well enough even for $r_a \sim 1$.

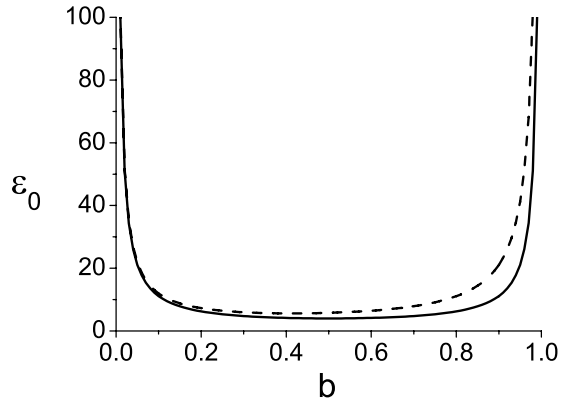

Fig. 2. Phase diagram: ε_0 vs. b. Top curve: $r_a = 0.001$ and down curve: $r_a = 1$, $\alpha = 0.4$.

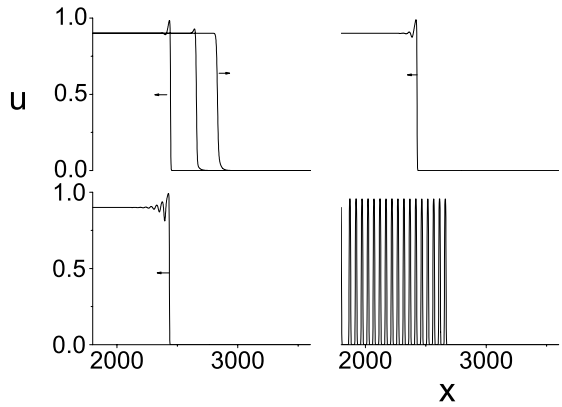

Fig. 3. Fronts solutions for different values of the intensity of interaction ($10 = L_{\rm diff}$). Up left: right to left: $\varepsilon_0 = 5 - 7 - 15$, up right: $\varepsilon_0 = 18$, down left: $\varepsilon_0 = 20$ and down right: $\varepsilon_0 = 21$. Other parameters: $b = 0.9$ and $\alpha = 0.3$, $r_a = 1$. Arrow indicates the direction of movement and the absence of an arrow indicates the front is static.

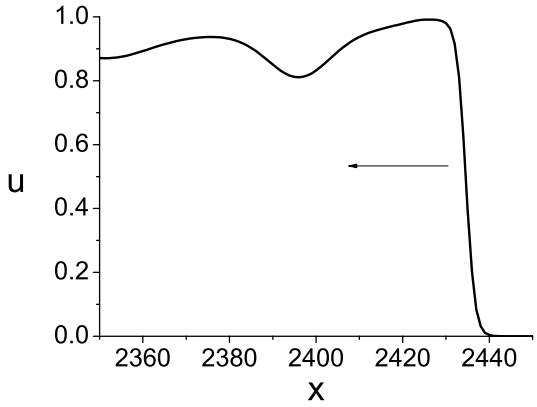

Fig. 4. Expanded view of fronts solutions for $\varepsilon_0 = 20$ ($10 = L_{\rm diff}$). Arrow indicates the direction of movement.

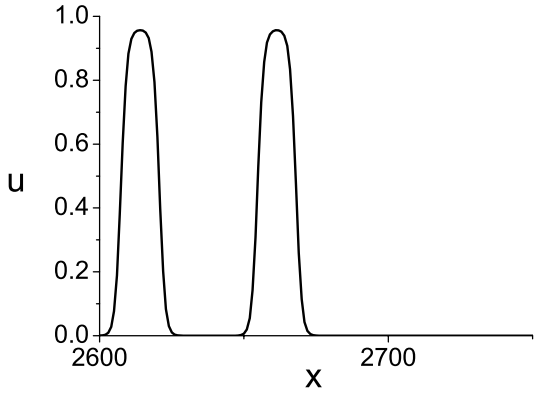

Fig. 5. Expanded view of static fronts solutions for $\varepsilon_0 = 21$ ($10 = L_{\rm diff}$).

It is clear that the solution $u = 0$ is always stable. If $u = b$ is destabilized by a non homogeneous perturbation, the system can evolve towards $u = 0$ or stabilized fronts, patterns or localized structures.

4 Fronts and patterns

Since equation (2) has front solutions which we already know (see expression (4)), we introduced these solutions in equation (5), we force the ends of the system in such a way as to hold the front ($u[\pm\infty] = b/0$ or $u[\mp\infty] = 0/b$) and follow its evolution in numerical form. For $\varepsilon_0 = 0$, the width of the front is of the order of the diffusion length $L_{\rm diff}$; but, when we introduce the effect of attractive forces, we also introduce another characteristic length (midrange of interaction: $L_{\rm diff} r_a$). The scale of observation and the value of both characteristic lengths suggest which parameter will be dominant (one of them, or both if their values are of the same order).

Figure 3 shows stationary profiles for a wide range of values of ε_0 (Figs. 4 and 5 show expanded views of two fronts to see the detail of the continuity of the curves). We mainly solved cases in which the midrange of the interaction is of the order of $L_{\rm diff}$ ($r_a \sim 1$). It is noted that for values of ε_0 between 0 and 5 (much below the stability limit curve of the stationary solution $u = b$) the profiles are similar to those already calculated for the case of absence of attractive forces (see expression (4)). But, while for $\varepsilon_0 = 0$ the front is static if $\alpha = \alpha_e = 0.5$, when ε_0 increases, the static adversity α_e decreases noticeably (this happens even for values upon $\varepsilon_0 \simeq 8$).

Figure 6 shows ($\varepsilon_0 = 7$) a static front ($\alpha_e \simeq 0.247$) and two fronts moving in either direction ($\alpha = 0.246$ – survival – and $\alpha = 0.248$ – extinction). Then, for values of ε_0 between 8 and 20, the front always evolves towards extinction, even for $\varepsilon_0 = 20$, a value above the stability limit curve (SLCb), although close to it. As seen in Figure 3, for this range of values, an insipient oscillation arises immediately behind the front (on $u = b$) that is dampened over a short distance. This oscillation grows strongly as ε_0 increases. Then, when ε_0 reaches 21, profiles change abruptly. In this last case ($\varepsilon_0 = 21$) the front is static and separates a pattern of extinction, circumstances in which the midrange of the interaction becomes the dominant parameter. Now we present a simple calculation applicable to the observed case when $\varepsilon_0 < 8$ and later we will deal with the other more interesting case ($\varepsilon_0 > 8$).

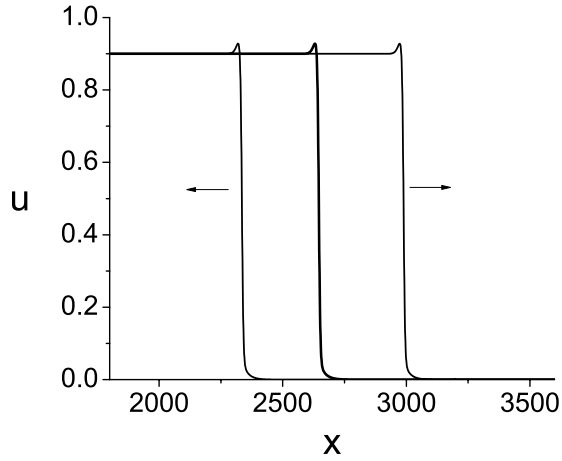

Fig. 6. Fronts solutions for three different values of α ($10 = L_{\text{diff}}$): left: $\alpha = 0.248$, middle: $\alpha = 0.246885$ and right: $\alpha = 0.246$, $\varepsilon_0 = 7$, $b = 0.9$ and $r_a = 1$. Arrow indicates the direction of movement and the absence of an arrow indicates the front is static.

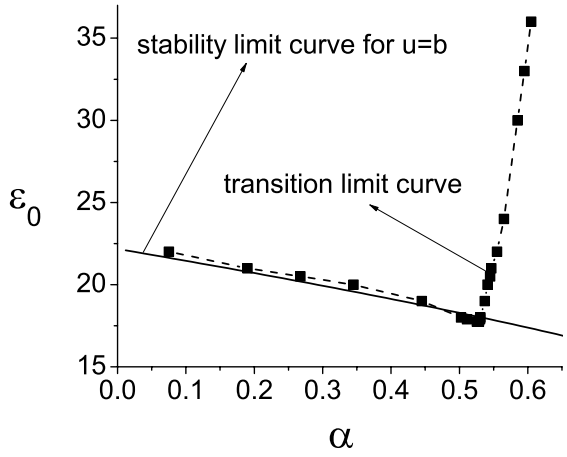

Fig. 7. Transition limit curve (TLC) and stability limit curve for $u = b$: ε_0 vs. α, $b = 0.9$ and $r_a = 1$.

Suppose a front that moves with a speed v. If we define $z = x - vt$, $E_p = \int F(u) D_{\text{eff}}(u) du$ and we apply these definitions to equation (6), then:

$$\partial_z \left[Ep(u) + \frac{D_{\text{eff}}(u)^2}{2} \partial_z u^2 \right] = -v D_{\text{eff}}(u) \partial_{zz} u.$$

Then, integrating over z between $-\infty$ ($u = b/0$) and $+\infty$ ($u = 0/b$) we get an expression similar to equation (3) which incorporates the effect of the attractive forces between individuals:

$$v = \pm 6 \frac{b^4 \left[24\alpha b\varepsilon (b - \frac{1}{3} + 1) - \frac{b\varepsilon(24+b)}{5} - \frac{1}{2} \right]}{\int_{-\infty}^{\infty} D_{\text{eff}}(u) (\partial_z u)^2 dz}. \quad (8)$$

Here we define $\varepsilon = \varepsilon_0 \frac{\partial_x U}{\partial_x u}$. For our analytical calculations, we are approaching $\frac{\partial_x U}{\partial_x u}$ with a form factor, so that we can consider ε as independent of u and x. Obviously, equation (8) does not enable us to calculate v, but from this we can infer that the Maxwell point is modified and we can understand the origin of this change. Although this expression does not accurately estimate under which conditions the adversity will prevail on survival ($\varepsilon_0 = 7$, analytical value: $\alpha_e = 0.3677$ and numeric value: $\alpha_e \simeq 0.247$), we know why when we increase ε_0 static adversity reduces.

Figure 3 shows, for $\alpha = 0.3$ and $\varepsilon_0 = 21$, a static front that separates a pattern of extinction. While for ε_0 lower, although always greater than 8 (for example $\varepsilon_0 = 18$) fronts are seen, that inexorably evolve toward extinction. This result leads us to explore the features of such a transition. Thus, we numerically calculate the corresponding limit curve for this transition (TLC), from which static pattern/($u = 0$) fronts begin to stabilize instead of ($u = b$)/($u = 0$) fronts moving toward extinction. Surprisingly we found a reentrant behavior with adversity, i.e., a window of values of α inside which these static pattern/($u = 0$) fronts stabilize. This indicates the seemingly counterintuitive result that with a small enough adversity, the system also evolves towards extinction.

Figure 7 shows such a transition limit curve, as well as the corresponding stability limit curve for the homogeneous solution $u = b$ (SLCb). We can observe that the branch corresponding to the small adversities that limits the transition between fronts is accompanied by the SLCb. This leads us to think that this limitation is associated to the destabilization of $u = b$. It is necessary that the homogeneous solution $u = b$ be destabilized to ensure that a pattern can be sustained against extinction on a static front. For values of ε_0 well above SLCb ($\varepsilon_0 \approx 25$, for $\alpha = 0.3$), we note that the pattern/extinction fronts stabilize quickly at a steady state, and this is done in a space period that corresponds to the optimal mode or is very close to the latter (k_m such that $\Omega_k(k_m)$ is a maximum). While below this value, the pattern that coexists with the extinction after quickly reaching a state; but this time, quasi-stationary (corrections on u of the order of $10^{-10}\delta t$, being δt the temporary step), is subjected to an intricate process of alternating long times characterized by imperceptible changes in the profile (with corrections on u in the same order as the already mentioned) and notable transformations carried out in a very short time. We believe that this process can be associated with the finiteness of the system. When we approached SLCb, the bandwidth that delimits the destabilizing modes is significantly reduced and could cause the profile to not quickly fit to one of those modes.

Figure 8 shows curves Ω_k vs. k for values of ε_0 between 21 and 30. As can be seen, although the optimal mode does not change too much with ε_0, the bandwidth of the destabilizing modes does. The dynamics that the limitation of the system causes can be interesting if we consider that real systems are finite.

Figure 9 shows a front previous to one of the mentioned transformations and another after this transformation.It is noted that one of the localized structures that make up the pattern has been eliminated, and that thereafter, the layout of these is more regular.

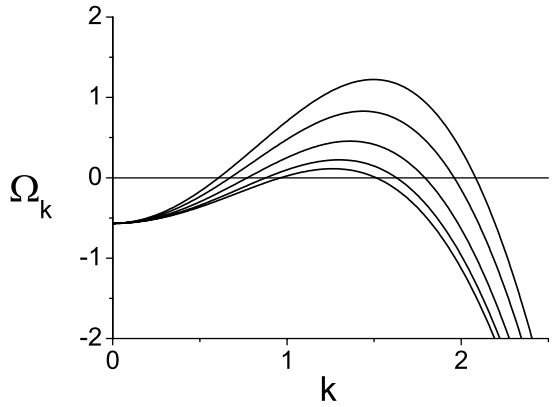

Fig. 8. Ω_k vs. k for square interaction. Top to down: $\varepsilon_0 = 30 - 26 - 24 - 22 - 21$. Other parameters: $r_a = 1$, $\alpha = 0.3$ and $b = 0.9$.

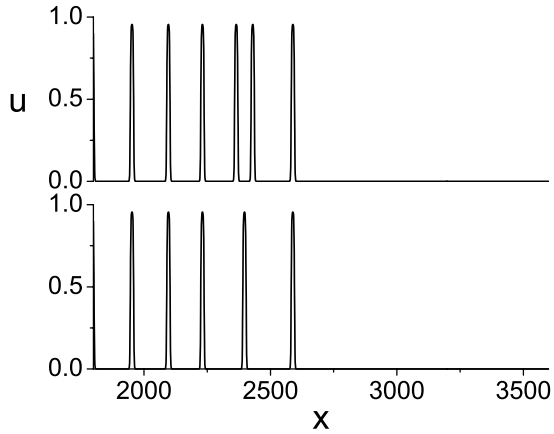

Fig. 9. Fronts solutions for $\varepsilon_0 = 22$ ($10 = L_{\text{diff}}$), $\alpha = 0.3$, $b = 0.9$ and $r_a = 1$. Up: previous to the transformation, down: after the transformation.

Figure 10 shows the details of what happened during the transformation. The above graph shows that two neighboring structures are slowly approaching. The middle graph shows a rapid transformation that occurs when the structures collide (the time involved in this process is much less than that corresponding to what is shown in the above graph). The graph below shows the result of the transformation. Only one of the two structures survives the encounter. In order to monitor in an objective and measurable manner, so much so this process as the degree of proximity to the stationary state we adopt the square of the area under the time derivative of the profile ($\dot{u}$) as a reference parameter. It is clear that this reference parameter must be zero for the steady state.

Figures 11 and 12, respectively, show the reference parameter following the evolution of the processes described above and an enlargement of the peak observed in the previous figure. We corroborate that the peak corresponds to the displayed transformation. It is noted that the ratio between the time of transformation (middle graph of Fig. 10) and that corresponding to the elapsed time during the whole process (between above and lower graph of Fig. 10) is of the order of 10^{-5}.

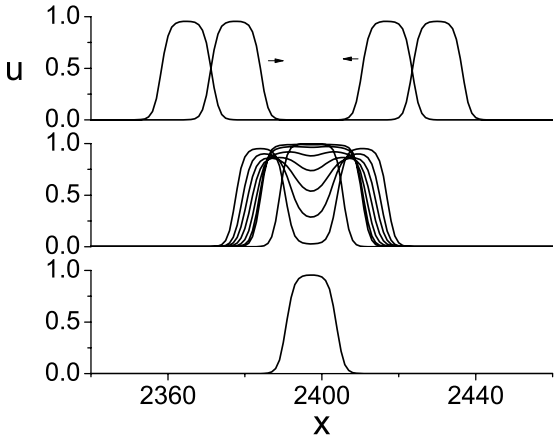

Fig. 10. Expanded view of fronts solutions for $\varepsilon_0 = 22$ ($10 = L_{\text{diff}}$), $\alpha = 0.3$, $b = 0.9$ and $r_a = 1$. Up: prior to the transformation, middle: during the transformation and down: after the transformation.

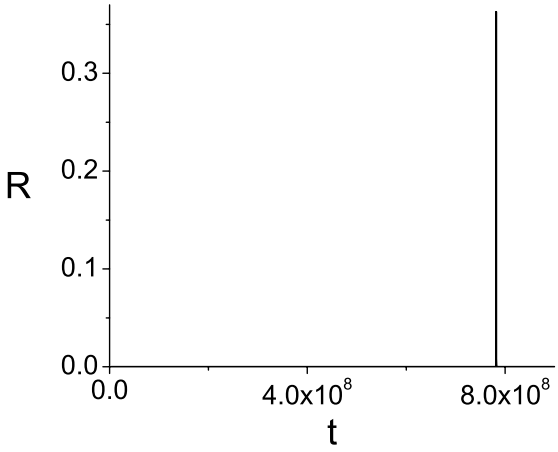

Fig. 11. Reference parameter versus time recording the transformation. t represents the number of steps used for numerical calculation (for this case, stages of $\delta t = 0.001$).

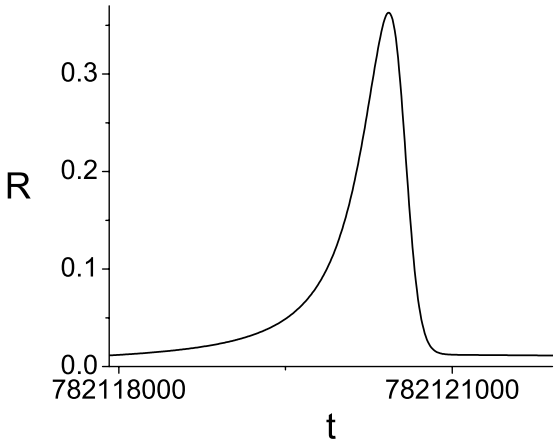

Fig. 12. Expanded view of reference parameter vs. recording the transformation. t represents the number of steps used for numerical calculation (for this case, stages of $\delta t = 0.001$).

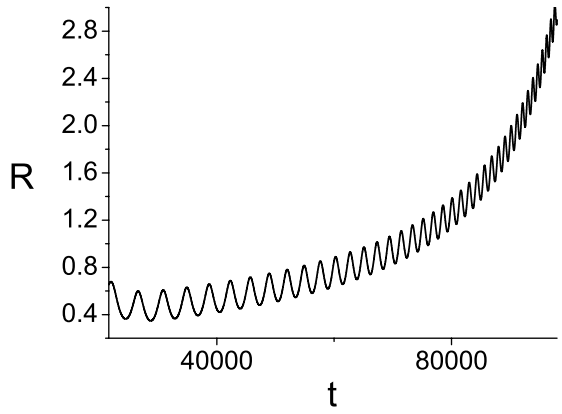

Fig. 13. Reference parameter R vs. time recording the slow movement of a structure. t represents the number of steps used for numerical calculation (for this case, stages of $\delta t = 0.001$). R is multiplied by 10^8.

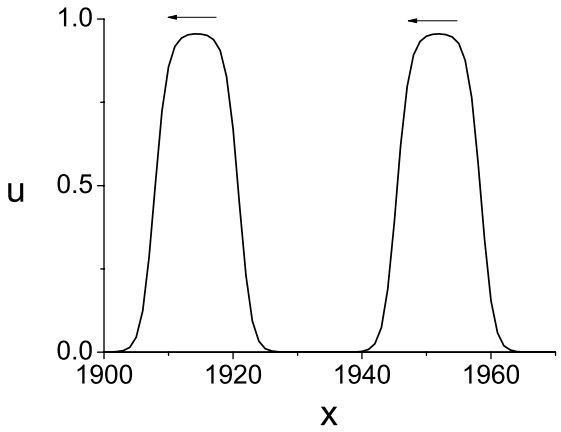

Fig. 14. Two stages of a structure moving that correspond with the beginning and the end of the curve shown in Figure 14. Right structure: $t = 21\,600\delta t$ and left structure: $t = 98\,000\delta t$.

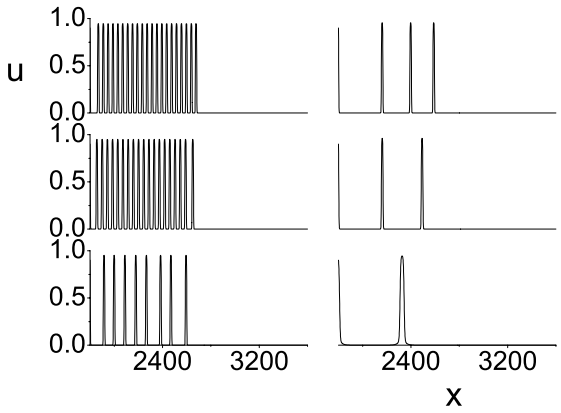

Fig. 15. Stationary Fronts and Localized structures solutions for different ε_0 excited from fronts ($10 = L_{\text{diff}}$); left up: $\varepsilon_0 = 30$, left middle: $\varepsilon_0 = 26$, left down: $\varepsilon_0 = 25$, right up: $\varepsilon_0 = 22$, right middle: $\varepsilon_0 = 18$, right down: $\varepsilon_0 = 7$; $\alpha = 0.3$, $b = 0.9$ and $r_a = 1$.

These rapid transformations are happening one by one during the evolution profile (but with very long intervals between them), causing the number of structures, over a very long time, to reduce. We emphasize that the profile is quasi-stationary; that is to say, except during the transformations, changes occur very slowly. These changes consist in the displacement of two structures that are approaching or of a single one that is moving. It is necessary to clarify that such structures are equal among themselves and do not change, neither their shape nor their size, while moving (only changes related to their movement and which are imperceptible if contrasted with those of the transformations); and also, that after a collision in which one of them is eliminated, the one that survives has the same shape and size as the previous one. It is clear that the above description relates to solitons. The slow movement of these solitons is recorded by the reference parameter as an extremely low oscillation of the amplitude mounted on a slower curve variation.

Figure 13 shows the details for this oscillation when only one structure is moving. We emphasize that during this process the only change to the profile is that associated with the structure that moves.

Figure 14 shows two stages of this movement that corresponds to the beginning and end of the curve shown in the figure above. We interpret that the oscillation of the reference parameter corresponds to increases and decreases in the population belonging to the structure or its immediate surroundings. This suggests that the movement is that of a worm, but while it moves, it varies in length.

Finally, after a long time the profile reaches a steady state consisting of a regular array of structures coexisting with extinction or, for lower intensity of interaction, only some localized structures distributed irregularly. We also found that depending on the mode of excitation of the front (introducing profiles obtained for other values of the parameters) the dynamic that is later generated can lead to a different result: a stationary stabilized pattern/extinction front, in another of the excitable modes (able to destabilize $u = b$) or one or two localized structure coexisting with extinction. This last can happen when the frequency of collisions between structures is so large (each collision eliminates one of them) that the number is not enough to construct a pattern with excitable modes.

Figure 15 shows a series of these already stationary solutions for values of ε_0 which range from 30 to 7 ($\alpha = 0.3$, $b = 0.9$ and $r_a = 1$). Some of them are fronts and other only localized structures irregularly distributed. In particular, the last curves ($\varepsilon_0 = 7$ and $\varepsilon_0 = 18$) may seem surprising, since for these values of intensity of interaction, the homogenous solution $u = b$ is stable and in addition we are under the TLC. To find this solution, we excite the fronts introducing into the system another solution front, which was obtained for a case above TLC. Done in this manner, the profile evolved in a similar way to the cases already described earlier (long periods with localized structures moving very slowly interspersed by eventual rapid transformations when two of them collide), although after a long time, the state declined toward some localized

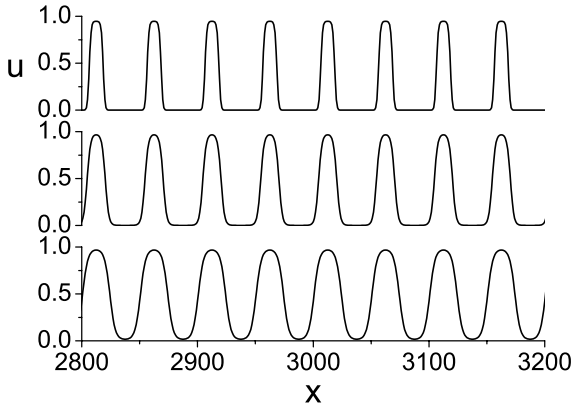

Fig. 16. Stationary patterns obtained by applying periodic conditions and provided that the spatial mode of the perturbation fits to the length of the system ($10 = L_{\text{diff}}$); up: $\varepsilon_0 = 30$, from a small spatially harmonica perturbation of solution $u = b$. Middle: $\varepsilon_0 = 14$, from profile of those obtained for the values of the parameters above SLCB. Down: $\varepsilon_0 = 9$, from profile same as the previous. Other parameters: $b = 0.9$, $\alpha = 0.3$ and $r_a = 1$.

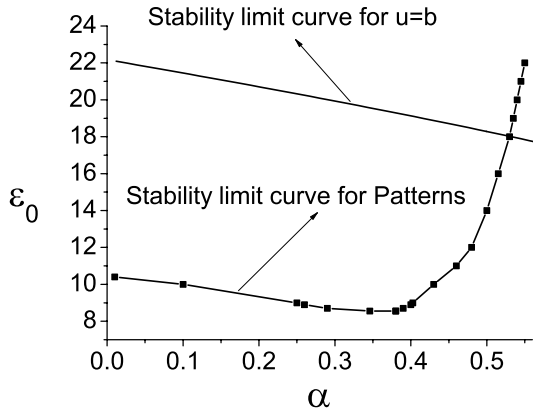

Fig. 17. Stability limit curve for patterns and stability limit curve for $u = b$: ε_0 vs. α, $b = 0.9$ and $r_a = 1$.

structures (above a given value of ε_0) or extinction (below this value).

We also try to excite patterns. To do so, we introduce a small spatially harmonic perturbation on $u = b$ selected from among the band of excitable modes ($\Omega_k(k) > 0$) and apply periodic boundary conditions. For values of parameters above TLC (see Fig. 7) and hence also the SLCB, provided that the spatial mode of the perturbation fits to the length of the system, a pattern quickly stabilized with the same excited mode.

Figure 16 shows stationary patterns for different ε_0. As can be seen, the structures that make up the patterns show differences between them. In particular, for ε_0 large, these are narrower and separated by a greater unpopulated space. While when ε_0 is reduced unpopulated spaces become narrower and the pattern takes on a more harmonic profile. In the figure, two of the three patterns that are displayed correspond to values of the parameters below SLCB. These last were excited by entering a profile of the obtained for values of the parameters above SLCB into a similar initial condition. That is to say, for this region of parameters, in addition to the two homogeneous solutions, stable patterns can also occur.

Figure 17 shows a curve (ε_0 vs. α) that indicates the region of parameter values where one of these patterns can stabilize.

Generally, when applying periodic boundary conditions, it is implicitly assumed that the system is large enough to qualify as infinite. This means that there are no limitations on the excitation of modes by the size of the system. However we thought it interesting to study what happens when one excites the system by inserting a small spatially harmonic perturbation, also about $u = b$, but with a mode that does not fit the length of the system and values of ε_0 near SLCB. As we expected, based on the results obtained for fronts, it was a more complex dynamic. Above a certain value of the intensity of interaction ($\varepsilon_0 \approx 26$ for $\alpha = 0.3$) a pattern stabilizes quickly (though not as much as in the previous case) in an excitable mode usually different from that of the perturbation and with some minor regularity defects. However, below this value of ε_0, depending on the mode of the excitation, different evolutions can occur. If such a mode does not fit the length of the system, what results is: first, in a short initial time, a self-constructing pattern occurs with characteristics similar to the previous but not steady. Later two fronts between patterns emerge (different values of k) that are propagated from the ends/center (k of the stationary profile) toward the center/ends (k of initial pattern) of the system. The mode k of the stationary pattern is included in a slightly enlarged band of excitable modes (it can be a stabilizing mode to just outside that band).

Figure 18 shows different stages in the evolution of one of these fronts. The dynamics adds another feature for even lower ε_0 ($\varepsilon_0 \approx 22/24$ for $\alpha = 0.3$) and same conditions as above. After the spread of the fronts, the state of the patterns remains as quasi-stationary. What follows is similar to that described for fronts under the same conditions: a quasi-stationary state characterized by slow-moving structures interrupted by eventual collisions, after which, only one of them survives. Finally, stabilizing the pattern in excitable mode (including those outside the band, but close to the edge) or stabilizing a few localized structures arranged irregularly.

Figures 19 and 20, respectively, show three profiles corresponding to the first stage of the propagation front and six profiles corresponding to the second stage described. Depending on the excitation mode, it may also occur that the phenomena described as two successive stages occur simultaneously. That is, at the same time that the fronts propagate collisions also occur between structures in the profile away from the fronts. As before, we believe that these dynamic changes are associated with the size of the bandwidth of excitable modes. When the bandwidth is narrower the result becomes more dependent on the limitations imposed by the finiteness of the system and therefore, increases the possibility of a more complex

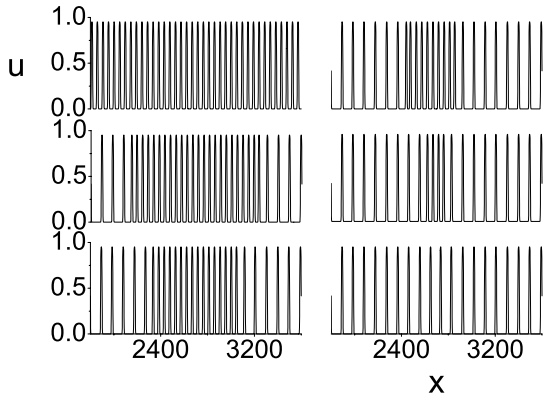

Fig. 18. Different stages of evolution for pattern fronts by applying periodic conditions, provided that the spatial mode of the perturbation does not fit to the length of the system and excited from a small spatially harmonica perturbation of solution $u = b$ ($10 = L_{\rm diff}$); left up: $t = 9 \times 10^8 \delta t$, left middle: $t = 207 \times 10^8 \delta t$, left down: $t = 279 \times 10^8 \delta t$, right up: $t = 369 \times 10^8 \delta t$, right middle: $t = 414 \times 10^8 \delta t$, right down: $t = 495 \times 10^8 \delta t$ (stationary state). Parameters values: $\varepsilon_0 = 25$, $b = 0.9$, $\alpha = 0.3$ and $r_a = 1$.

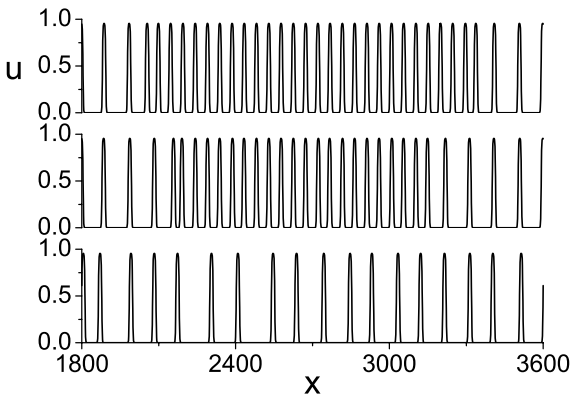

Fig. 19. Different stages of evolution for pattern fronts by applying periodic conditions, provided that the spatial mode of the perturbation does not fit to the length of the system and excited from a small spatially harmonica perturbation of solution $u = b$ ($10 = L_{\rm diff}$); up: $t = 18 \times 10^8 \delta t$, middle: $t = 27 \times 10^8 \delta t$, down: $t = 54 \times 10^8 \delta t$ (quasistationary state). Parameters values: $\varepsilon_0 = 22$, $b = 0.9$, $\alpha = 0.3$ and $r_a = 1$.

dynamics than that which can change the result of patterns to localized structures. It is clear that forcing the periodicity of a finite system can represent an artificial situation, however, it seems to us that the dynamics that this generates is rich enough to deserve mention. A more realistic situation is to set boundary conditions fixed for u (any value between 0 and 1). So therefore, we numerically solved cases like these and got the same results as those described above. We highlight that when referring to the finiteness of the system we are not saying that the complexity of the described dynamics is very sensitive to the size of the system. We doubled and quadrupled the size of the system and we did not appreciate loss of complexity in the dynamics. It seems that what triggered this dynamics, beyond the size of the system, is the mismatch of then non homogeneity with the boundary conditions.

5 Localized structures

The coexistence of patterns and homogeneous solutions suggest the possibility of localized structures can stabilize [33,34]. In the previous section we note some cases where quasi-stationary patterns or pattern/extinction front arise as numerical solutions of equation (5), but that in a very long time they slowly evolve toward stable localized structures with mobility (solitons) to finally be stationary. These types of solution for the original Nagumo model (see Eq. (2)) are not stable [28,29,32].

We propose a more in depth study, of the possibility that attractive interactions can stabilize localized structures.

To explore this possibility we did a rough calculation using a technique already known by applying the condition of solubility [28,29,32–34]. After a linearization of equation (6) is obtained: $\dot{\phi} = £\phi$, where ϕ is a non homogeneous small perturbation and £ a linear operator which has the form:

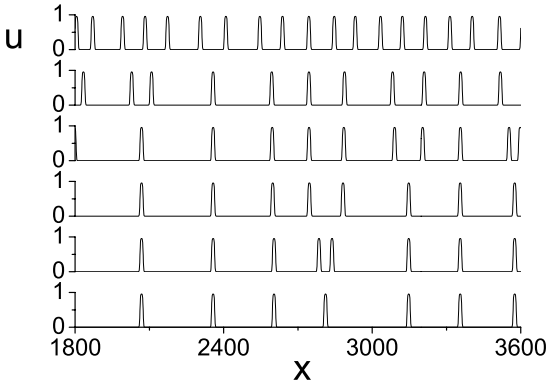

Fig. 20. Different stages of evolution for an array of localized structures originating from a quasi-stationary patterns by applying periodic conditions, provided that the spatial mode of the perturbation does not fit to the length of the system and excited from a small spatially harmonica perturbation of solution $u = b$ ($10 = L_{\rm diff}$); up to down: $t = 54 \times 10^8 \delta t$, $t = 108 \times 10^8 \delta t$, $t = 198 \times 10^8 \delta t$, $t = 288 \times 10^8 \delta t$, $t = 558 \times 10^8 \delta t$ and $t = 648 \times 10^8 \delta t$. Parameters values: $\varepsilon_0 = 22$, $b = 0.9$, $\alpha = 0.3$ and $r_a = 1$.

$$£ = \partial_u F^{u^s} + \partial_x \left[D^{u^s}_{\rm eff} \partial_x + \partial_u D^{u^s}_{\rm eff} \partial_x u^s \right],$$

representing u^s the stationary solution front of equation (6). For this calculation we again consider $\frac{\partial_x U}{\partial_x u}$ as a form factor, so that we can assume ε independent of u and x.

Since the operator £ accepts as eigenvectors to $\partial_x u^s$, with eigenvalue zero ($£\partial_x u^s = 0$); and that for values of ε_0 below the limit curve of stability corresponding to the homogeneous solution $u = b$ there are fronts that have the appearance of the solutions of equation (2), in this case, we can approximate $u^s \approx u^s \mp$ (see expression (4)) and

then apply the referred technique [28,29,33,34] to the case above.

Thus, we propose as an approximation for the localized structure: $u = u^s_+ + u^s_- - b + \overline{\phi}$, with $\overline{\phi} = \eta \partial_x u^s \mp$, being η a small parameter and

$$u^s_\mp = \frac{b}{2}\left[1 \mp \tanh\frac{b}{2\sqrt{2}}\left(x - x^\pm_f\right)\right].$$

By identifying with $x^\pm_f$, the position of each front, with $x^+_f > x^-_f$.

Then, we define the width of the localized structure as $\Delta = x^+_f - x^-_f$, and adopt $\Delta \gg L_{\text{diff}}$ and $\Delta \gg r_a$. This last enables us to approach: $u^s_\pm \simeq b[1 - e^{-\frac{b}{\sqrt{2}}(\Delta + x - x^\pm_f)}]$ in the environment of $x^\mp_f$, being $e^{-\frac{b}{\sqrt{2}}\Delta}$ as small as η. Also, as in the aforementioned reports [28,29,32], we considered $\alpha = \alpha_e + \delta\alpha$, with $\delta\alpha \sim \eta \sim e^{-\frac{b}{\sqrt{2}}\Delta}$.

Finally, introducing u in equation (6), applying the above considerations, and then the condition of solubility (taking into account that the eigenvectors $\partial_x u^s \mp$ only affect the environment of the fronts), we obtain:

$$\dot{\Delta} \simeq -2\sqrt{2}b\delta\alpha + 12\sqrt{2}b\left[\varepsilon b\frac{2.62 - 2b}{8} + \frac{3}{4}\alpha_e - \frac{9}{8}\right]e^{-\frac{b}{\sqrt{2}}\Delta}. \quad (9)$$

Then, since we are only interested in the role of the attractive forces in the stabilization of the localized structure, we consider the strongest approximation:

$$e^{-\frac{b}{\sqrt{2}}(\Delta + x - x^\pm_f)} \simeq e^{-\frac{b}{\sqrt{2}}\Delta}$$

and so,

$$\dot{\Delta} \simeq -2\sqrt{2}b\delta\alpha + \sqrt{2}b\left[\varepsilon b - 12(1 - \alpha_e)\right]e^{-\frac{b}{\sqrt{2}}\Delta}. \quad (10)$$

It can be seen that, indeed, the attractive forces tend to stabilize localized structures and succeed when ε is large enough. This is evidenced by the fact that conditions exist for a stationary solution Δ^s and the slope of $f(\Delta^s)$ is less than zero when this happens ($\dot{\Delta} = f(\Delta)$).

It is clear that the range of application of this result is limited by the assumptions made; nevertheless, it is a significant indication that the attractive forces may be sufficient to stabilize localized structures in the Nagumo dynamic.

It can be observed that the stationary solution corresponds to $\delta\alpha > 0$, which tends to cause the collapse of the fronts and therefore extinction. On the other hand, the effect of the attractive forces is to contain such a collapse, stabilizing the localized structure. While the dynamics of Nagumo drives individuals toward extinction, they achieve survival by trying to stay in the heart of the structure (a state energetically favorable if we compare it with individuals located at the interface).

In references [28,29,32], it was reported that the incorporation of a non local term to the Nagumo nonlinearity causes rich dynamics that among other things

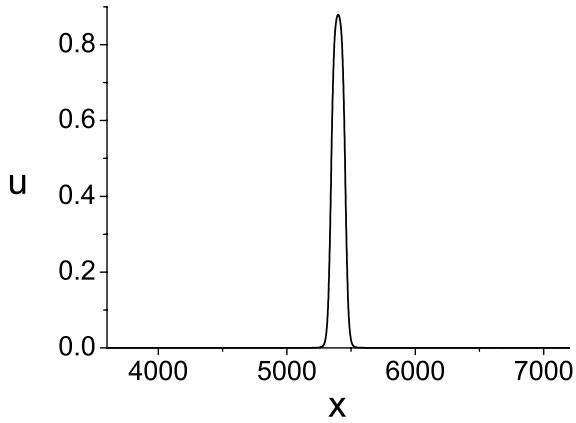

Fig. 21. Localized structure just above its stability limit curve: u vs. x ($40 = L_{\text{diff}}$); $r_a = 2.1$, $\varepsilon_0 = 15.2$ and $\alpha = 0.5$.

generates the stabilization of localized structures. In particular, the non-locality affects the cubic term of Nagumo non-linearity. This term expresses the Allee effect [2–4] (competition for resources that causes saturation in the population density).

In the present report, we show the effect of a phenomenon contrary to the competition: a collaboration (attraction between individuals). We show how this phenomenon drives a current $J_A(x)$ (which also includes a non-local term $-\partial_x U$) that leads to similar phenomena of self-organization.

It is important to emphasize that for the present model self-organization is caused by a current driven by attractive forces and not by non locality of the phenomenon. In fact, in the approximation used the non-local effect has been minimized to a mere constant form, being the effect relevant to the stabilization of the localized structures, the attractive forces in opposition to the phenomenon of diffusion. This view is reinforced by the fact that for the model that is being reported in references [28,29], the results strongly depend on the type of kernel used to describe the non-locality of the phenomenon [35], while that for the present model this is not the case.

To check this result, starting from $u = u^s_+ + u^s_- - b$, we numerically calculate the evolution of $u(x)$, whose dynamics is governed by equation (5). Thus, we find a region of parameters within which localized structures stabilize.

Figure 21 shows a case just above the limit curve (SLCLS) below which these structures are destabilized and evolve rapidly toward extinction.

Figure 22 shows an expanded view of various localized structures just above and following the course of such limit curve for different values of $r_a \sim 1$. It can be observed that when the midrange of interaction increases the localized structures become taller and grow wider.

Figure 23 shows another expanded view of various localized structures, now $r_a = 1$ and $\alpha = 0.5$ remain constant, ε_0 increasing from 13.8 to 30. It can be seen that, under these conditions, when ε_0 increases, the localized structures are more square and taller, although their

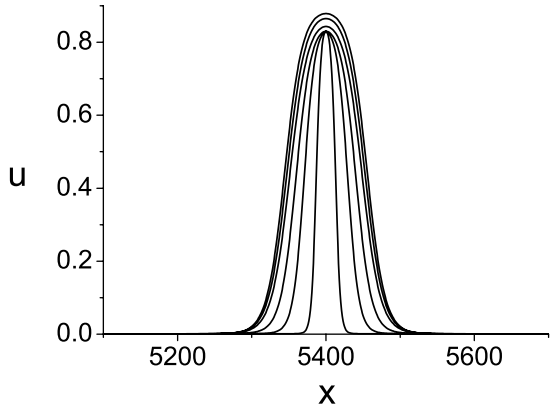

Fig. 22. Expanded view of localized structures just above its stability limit curve: u vs. x ($40 = L_{\text{diff}}$); $\alpha = 0.5$. Top to down: $r_a = 2.1 - \varepsilon_0 = 15.2$, $r_a = 1.95 - \varepsilon_0 = 13.84$, $r_a = 1.8 - \varepsilon_0 = 13.00$, $r_a = 1.5 - \varepsilon_0 = 13.15$, $r_a = 1.1 - \varepsilon_0 = 13.66$, $r_a = 0.5 - \varepsilon_0 = 14.8$.

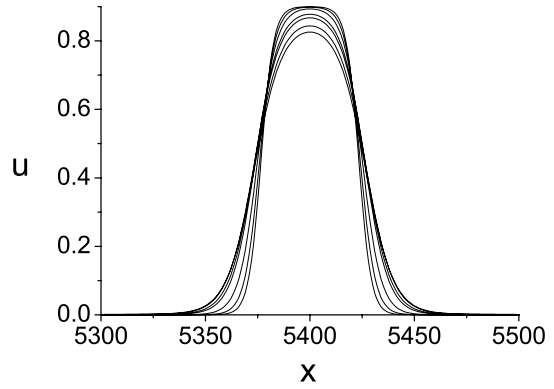

Fig. 23. Expanded view of localized structures for different ε_0 starting from its stability limit curve: u vs. x ($40 = L_{\text{diff}}$); $b = 0.9$ and $\alpha = 0.5$, $r_a = 1$, and down to top: $\varepsilon_0 = 13.8 - 14 - 15 - 20 - 25 - 30$.

average width does not vary significantly. As expected, the last depends on the midrange of the interaction. In all observed cases the average width of the localized structure was approximately equal to the double of r_a.

Figure 24 shows the limit curve (SLCLS) for a wide range of values of r_a. This figure also shows the stability limit curve (LCb) corresponding to the solution $u = b$. It can be seen that, for smaller values of r_a, localized structures are stabilized only above this last curve (SLCb), while that for higher values of r_a such structures can stabilize below and above this curve.

Figures 25 and 26 show the corresponding curves (SLCLS) by varying the parameters b and α, together with the stability limit curves corresponding to $u = b$. Here we can also see that both limit curves intersect. If b or α are sufficiently large, localized structures can stabilize below and above the stability limit curve for $u = b$.

We also calculate cases with r_a very small ($r_a \sim 0.001$) that, of course, required much more computation time. As Figure 24 suggests, it was necessary to consider a value

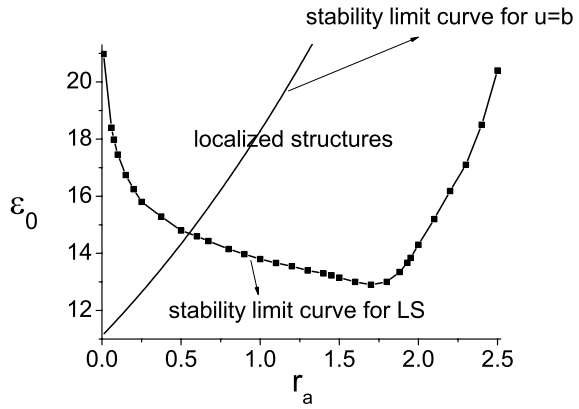

Fig. 24. Phase diagram for localized structures: ε_0 vs. r_a; $b = 0.9$ and $\alpha = 0.5$.

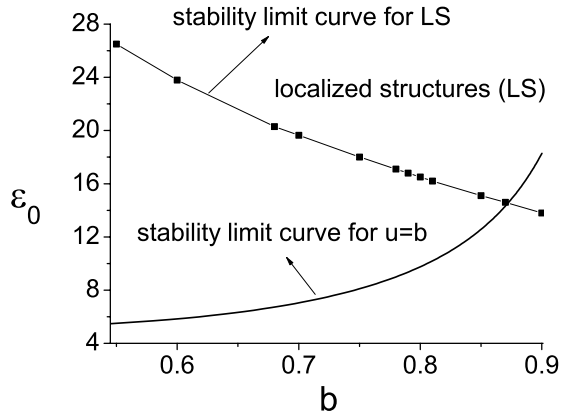

Fig. 25. Phase diagram for localized structures: ε_0 vs. b; $\alpha = 0.5$ and $r_a = 1$.

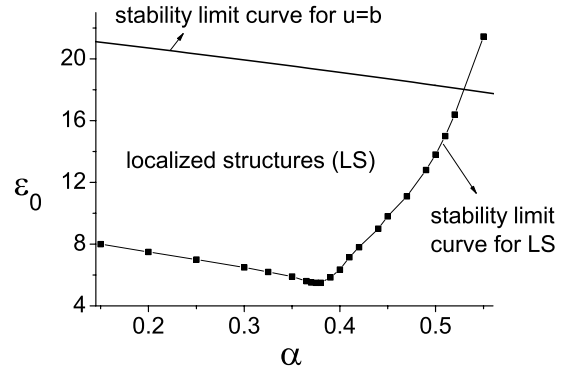

Fig. 26. Phase diagram for localized structures: ε_0 vs. α; $b = 0.9$ and $r_a = 1$.

of strength of attractive forces large enough to achieve a stable localized structure ($\varepsilon_0 = 30$).

Figures 27 and 28, respectively, show one of these cases, and an expanded view of the same case added to another with different adversity ($\alpha = 0.4$ and $\alpha = 0.5$). A tendency to decrease the height of the peak with the increase of the adversity can be observed. Already for $\alpha = 0.7$ localized structures destabilize and evolve towards extinction.

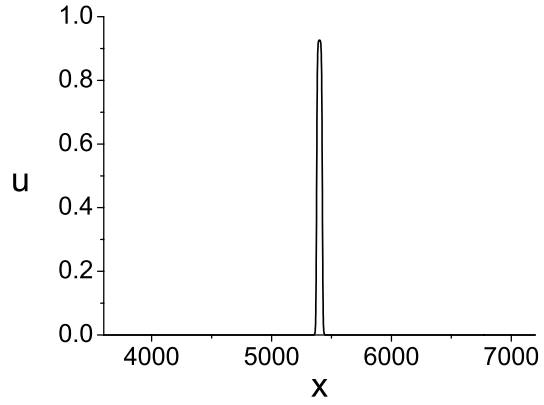

Fig. 27. Localized structure: u vs. x ($40\,000 = L_{\rm diff}$); $r_a = 0.001$, $\varepsilon_0 = 30$, $b = 0.9$ and $\alpha = 0.4$.

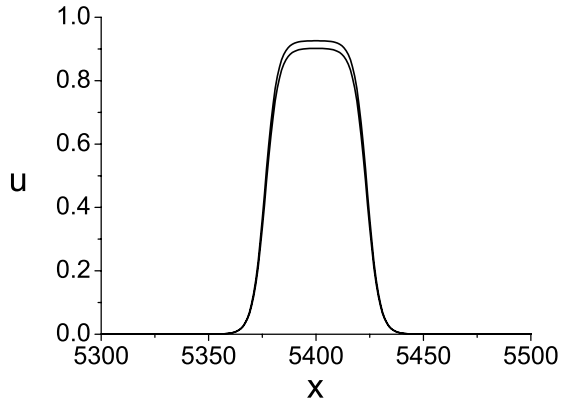

Fig. 28. Expanded view of localized structures for two different α: u vs. x ($40\,000 = L_{\rm diff}$); $r_a = 0.001$, $\varepsilon_0 = 30$, $b = 0.9$ and, top to down: $\alpha = 0.4$ and $\alpha = 0.5$.

Another goal that we set for ourselves was to study the possibility of more complex localized structures, i.e., constituted by multiple simple structures. To do this, we again excite the system starting from $u = u^s_+ + u^s_- - b$, but increasing Δ. To achieve multiple structures we had to consider values of ε_0 higher than those we were using ($\varepsilon_0 \geq 40$).

Figure 29 shows several solutions for the same set of values of the parameters that characterize the model. To obtain these different solutions, we only changed Δ, which is a parameter that only characterizes the profile with which the system is excited.

6 Conclusions

As mentioned in the introduction, a crisis can give origin to gregarious behavior. Several studies support the fact that this type of behavior is based on physically or chemically specific mechanisms of each species [21–24]; but that, generically, it can be represented as a force that induces individuals to join [27]. We mathematically represent this effect and add it to a system governed by the Nagumo dynamic. Since the agglutinating current caused by such

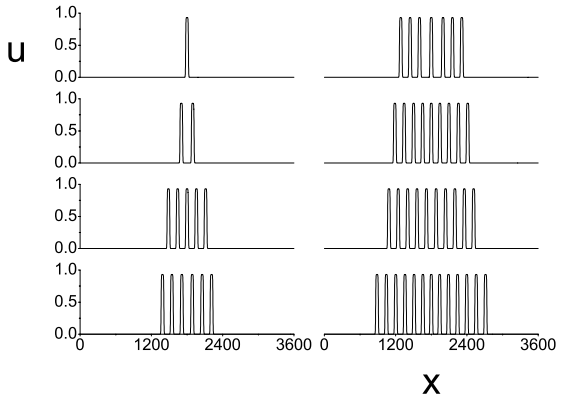

Fig. 29. Multiple localized structures excited from $u = u^s_+ + u^s_- - b$ with different values of Δ ($40 = L_{\rm diff}$). Left top to down: $\Delta = 100, 200, 400, 500$. Right top to down: $\Delta = 600, 700, 800, 1000$; $r_a = 1$, $\varepsilon_0 = 40$ and $\alpha = 0.3$.

attractive forces opposes the diffusion process, if the former are sufficiently strong, they can sustain the growth of a non homogeneous fluctuation. We show that this is indeed true by carrying out the corresponding analysis of stability. Actually there is a band of destabilizing modes of the homogeneous solution $u = b$.

Hasty vision could lead us to think that the existence of these modes could promote extinction. It was quite the opposite. The attractive forces promoted the stabilization of static pattern/extinction fronts, patterns and localized structures of various complexities.

It is clear that if the homogeneous solution $u = b$ is stable, the attractive forces between individuals do not promote a benefit for survival. However, a crisis can cause such large fluctuations, that they can destabilize a homogeneous solution. In this case, individuals who have a mechanism of mutual attraction can survive by forming patterns and localized structures that coexist with extinction or other contexts. Moreover, we show that if the attraction between them is not sufficiently strong, there is a dynamic in which localized structures compete for subsistence.

In particular, we show how these structures (solitons) move to attract each other, but when they collide, after that, only one structure survives. We cannot say that the structure that survives is exactly one of those prior to the collision, rather it seems to be a new structure, product of the other two and identical to the previous.

In addition, previous to this dynamic, depending on excitation, we also observed fronts between patterns characterized by different modes k. We believe that this dynamic is associated with the finiteness of the system, i.e., that it is driven by the need that the structures fit into the system available for the life of the population. However, if the system is infinite and solitons are close enough, they also attract and finally they coalesce (numerical tests were carried out to check this).

Similar phenomena have been observed in other contexts, particularly in parametrically driven systems [36]. However, that is a different phenomenon than what is

reported in this paper. First of all, they do not belong to the same class of universality. This is reflected in the remarkable differences between the equations that describe both dynamics. In reference [36] the parametric excitation of the solitons is strictly necessary for these to arise and be stabilized. In our model the solitons arise spontaneously by the perturbation of a homogeneous solution with a weak spatial oscillation and then, they are promoted and stabilized by the attractive forces between individuals. In [36], intrinsic frequencies strongly related to the response that is given by the system due to the effect of parametric excitation, are reported. In our model, there are no such frequencies; there are a band of excitable modes affected by the attraction between individuals. What they have in common is that in both cases the solitons interact among themselves in a similar way. There are pairs that are attracted to each other which slowly approach and then coalesce, with finally, only one identical to the previous ones.

Summarizing, we consider a population of individuals governed by the dynamics of Nagumo model and we incorporate a current that expresses attraction between individuals. After a stability analysis, we calculate the dynamics of this system and as a result get static pattern/extinction fronts for a continuous range of values of the adversity, as well as solitons coexisting in the same system. Before achieving such coexistence we observed a surprising dynamic that demonstrated to us that these attract each other until only one of the two survives after a collision. The movement of these solitons is very slow in comparison with the duration of each collision. After a long period of time, during which several of these collisions occur, finally, a steady state is reached in which the surviving solitons coexist.

I acknowledge financial support from CONICET, Argentina; and UNMdP, Argentina, EXA603/12. I also acknowledge to Srta. Natalia Bettiol for great help with the English language.

References

1. J.D. Murray, *Mathematical Biology*, 2nd edn. (Springer-Verlag, New York, 1993)
2. W.C. Allee, *Animal Aggregations: A Study in General Sociology* (University Chicago Press, Chicago, 1931)
3. W.C. Allee, *The Social Life of Animals* (Beacon Press, Boston, 1938)
4. B. Perthame, *Transport Equations in Biology, Frontiers in Mathematics* (Springer-Verlag, New York, 2008)
5. A.M. Moya, in *La génesis de la complejidad biológica*, edited by E. Molina (Universidad de Zaragosa, Spain, 1996) pp. 111–122
6. M.E. Boraas, D.B. Seale, J.E. Boxhorn, Evolutionary Ecology **12**, 153 (1998)
7. A.W. Murray, J.H. Koschwanez, K.R. Foster, PLoS Biol. **9**, e1001122 (2011)
8. T. Pitcher, A. Magurran, I. Winfield, Behav. Ecol. Sociobiol. **10**, 149 (1982)
9. B. Partridge, J. Johansson, J. Kalish, Environ. Biol. Fishes **9**, 253 (1983)
10. F. Fish, J. Experimental Zoology **273**, 1 (1995)
11. H. Milinski, R. Heller, Nature **275**, 642 (1978)
12. G. Roberts, Animal Behaviour **51**, 1077 (1996)
13. S. Lima, Animal Behaviour **49**, 11 (1995)
14. W.D. Hamilton, J. Theor. Biol. **31**, 295 (1971)
15. G. Turner, T. Pitcher, American Naturalist **128**, 228 (1986)
16. G.D. Ruxton, J. Krause, D.I. Rubenstein, J. Fish Biol. **52**, 494 (1998)
17. R.D. Alexander, Ann. Rev. Ecol. Syst. **5**, 325 (1974)
18. B.C.R. Bertram, in *Living in groups: predators and prey, Behavioral Ecology*, edited by J.R. Krebs, N.B. Davies, 1st edn. (Blackwell Scientific, Oxford, 1978), pp. 64–96
19. D.I. Rubenstein, Perpesptives in Ethology **3**, 205 (1978)
20. D.J. Hoare, I.D. Couzin, J.G.J. Godin, J. Krause, Animal Behaviour **67**, 155 (2004)
21. M.V. Abrahams, P.W. Colgan, Environ. Biol. Fishes **13**, 195 (1985)
22. B. Partridge, T. Pitcher, M. Cullen, J. Wilson, Behav. Ecol. Sociobiol. **6**, 277 (1980)
23. S.M. Rogers, T. Matheson, E. Despland, T. Dodgson, M. Burrows, S.J. Simpson, J. Exp. Biol. **206**, 3991 (2003)
24. G.D. Ruxton, T.N. Sherratt, Proc. R. Soc. B **273**, 2417 (2006)
25. J.T. Sumpter, Philos. Trans. R. Soc. B **361**, 5 (2006)
26. D. Helbing, P. Molnár, Phys. Rev. E **51**, 4282 (1995)
27. S.E. Mangioni, Physica A **391**, 113 (2012)
28. D. Escaff, Ph.D. thesis, Facultad de Ciencias de la Universidad de Chile, Santiago, 2006
29. M.G. Clerc, D. Escaff, V.M. Kenkre, Phys. Rev. E **72**, 056217 (2005)
30. S.E. Mangioni, R.R. Deza, Phys. Rev. E **82**, 042101 (2010)
31. S.E. Mangioni, R.R. Deza, Physica A **391**, 4191 (2012)
32. M.G. Clerc, D. Escaff, V.M. Kenkre, Phys. Rev. E **82**, 036210 (2010)
33. P. Coullet, Int. J. Bifur. Chaos Appl. Sci. Eng. **12**, 2445 (2002)
34. P. Coullet, C. Riera, C. Tresser, Phys. Rev. Lett. **84**, 3069 (2000)
35. D. Escaff, Eur. Phys. J. D **62**, 33 (2011)
36. M.G. Clerc, S. Coulibaly, L. Gordillo, N. Mujica, R. Navarro, Phys. Rev. E **84**, 036205 (2011)